Jordan Journal of Civil Engineering, Volume **16**, No. **4**, **2022**

Linear and Geometrically Non-linear Free in-Plane Vibration of a Circular Arch with Damages

Omar Outassafte [1,2)*], ***Ahmed Adri*** [1)], ***Yassine El Khouddar*** [1,2)], ***Issam El hantati*** [1,2)], ***Said Rifai*** [1)] ***and Rhali Benamar*** [3)]

[1)] Laboratory of Mechanics Production and Industrial Engineering (LMPGI), High School of Technology (ESTC), Hassan II University of Casablanca, Route d'El Jadida, Km 7, 8012 Oasis, Casablanca, Morocco.
[2)] Doctoral Studies Center of National High School of Electricity and Mechanics (ENSEM), Hassan II University of Casablanca, Route d'El Jadida, Km 7, 8018 Oasis, Casablanca, Morocco. * Corresponding Author.
[3)] EMI-Rabat, LERSIM, Modelling and Scientific Computing Department, Mohammed V University in Rabat, Agdal, Rabat, Morocco.

ABSTRACT

The geometrically non-linear free in-plane vibration of a circular arch with damages is studied in this paper. The structure damage can be due to several factors, such as shocks, heat treatments, fabrication processes or large-amplitude vibrations. The purpose of the current study is to examine the vibratory behavior of curved beams. In this investigation, the damage is modeled as a rotating elastic spring linking two adjacent arch sections. The theoretical formulation is developed on the basis of the von Kármán non-linearity assumptions and the Euler-Bernoulli beam theory. After solving the linear problem, the non-linear equilibrium equations are determined using Hamilton's principle. An approximate method called the second formulation is used to solve the non-linear algebraic system obtained. The effects of varying the position, damage intensity and number of damages on the linear and non-linear dynamic behaviors of the arch are investigated.

KEYWORDS: Geometrically non-linear vibration, Damages, Rotational elastic spring, Hamilton principle, Second formation.

INTRODUCTION

Arch vibration has attracted the attention of a large number of researchers worldwide, due to the wide application of this kind of structure in different industrial fields, such as aeronautics, mechanical engineering and civil engineering. The immediate reason for this growing interest is the ability of these structures to transfer loads through the combined action of bending and stretching for in-plane deflections. Furthermore, there is an increasing need to design and create an infrastructure that combines aesthetic characteristics with mechanical properties to ensure good stability over a long period and a high resistance to various external or internal forces, such as the movement of vehicles in the case of bridges or wind for large buildings. Moreover, conventional structural-stress analysis can lead to inaccurate safety conclusions if damages, which occur very often, are ignored. These damages, which are considered mainly as section damages, create discontinuities in the bending stiffness of the material and cause damping changes at the damaged locations. Therefore, several studies have been carried out to improve analytical or numerical approaches that allow the prediction and identification of the locations and sizes of cracks. Yang et al. (2018) have developed an energy-based calculation model to analyze the influence of damage on the vibrations of a beam with an open crack. Papaeconomou and Dimarogonas (1989) improved the transfer matrix and applied it to estimate the dynamic behavior of simply cracked beams in free vibration. The results showed that the resonance frequencies and vibration modes are

Received on 12/3/2022.
Accepted for Publication on 26/6/2022.

considerably influenced by the presence of moderate cracks. Galerkin-type solution for the one-dimensional Bernoulli-Euler equation for a cracked beam was proposed, where the results obtained for the first three natural frequencies and mode shapes were found to be in good agreement with the finite-element analysis and experimental results available in the literature. Khiem and Lien (2002) studied the response of a beam having an arbitrary number of cracks to external load using the dynamic stiffness method (DSM). For the prediction of changes in flexural vibration of a simply supported beam with a single open-edge or a double-edge open surface crack, a numerical solution was presented by Chondros et al. (1998). The results were confirmed by experiments on aluminum beams with fatigue cracks and with analytical results obtained from the theory (Christides and Barr, 1984). According to Chondros and Dimarogonas (1980), the problem of beams with localized damages with various depths may be modelled by two or more independent beams attached by a torsional spring at the cracked sections. In order to detect the crack location and quantification of damage magnitude in a uniform beam under simply supported or cantilever boundary conditions, Liang et al. (1991) developed a method based on the measurement of the natural frequencies of the structures. Sinha et al. (2002) presented a non-intrusive and non-destructive method that estimates the locations and depths of cracks in beams employing the solution of an inverse-vibration problem. Altunışık et al. (2019) presented a study to demonstrate the effectiveness of modal-curvature and modal-flexibility methods for damage detection on a cantilever steel beam with a circular hollow section and multiple cracks. The results have been validated based on the experimental vibration data. Zare (2018) studied the problem of crack detection in a curved beam using an inverse method. The determination of natural frequencies was numerically performed using the quadrature differential element method. Employing an approach which allows the estimation of the strain-energy release rate, Zare (2020) investigated the out-of-plane vibration of a cracked curved beam on an elastic foundation with a rectangular cross-section.

The vibration of arches has been the subject of much research, such as the book by Henrych (1981), which deals with the theory of arched structures and frames. In order to obtain accurate values of free vibration frequencies, Chidamparam and Leissa (1993) employed the Galerkin method, including polynomial test functions that satisfy geometrical boundary conditions. Auciello and De Rosa (1994) applied the Rayleigh-Ritz method to investigate the in-plane vibration of arches with a non-uniform thickness in which the effects of axial extension, shear deformation and rotational inertia are considered. Zhao and Kang (2008) studied the free in-plane vibration of a circular arch with a uniform and discontinuously varying cross-section using the transfer-matrix method. The effects of damping, axial extension, transverse shear deformation and rotational inertia were neglected. The results showed that for all modes, the natural frequencies show an important increase for the arch cable with an increase in the stiffness, number and location angle of the cable. On the contrary, the natural frequencies showed clear decreases with the increase in the opening angle and the arc length. Irie et al. (1983) presented the natural frequencies for the in-plane vibration of uniform arches with circular cross-section under various types of boundary conditions. Tüfekçi (2001) found an exact solution of the equations governing the motion of curved circular beams with uniform cross-sections, where the effects of transverse shear, axial extension and rotary inertia were taken into account. Laura and de Irassar (1988) determined the first two natural frequencies of simply supported and clamped circular symmetrical arches the thickness of which varies linearly and for arches the thickness of which varies discontinuously, which carry concentrated masses. Babahammou and Benamar (2020) improved a semi-analytical solution for the free in-plane vibration of inextensible circular arches which have uniform cross-sections and are elastic against the rotation at two ends. Using a finite-element method, Krawczuk and Ostachowicz (1997) demonstrated the effects of crack position and location of a curved beam with a transverse open crack on one edge, on the natural frequencies as well as on the mode shapes. The results showed that the reduction of the in-plane natural frequencies of the arch is a function of the depth and location of the crack. Cerri et al. (2008) presented the experimental results of the dynamic behavior of undamaged and damaged circular arches, then compared them with those of analytical methods. Ja'E (2018) performed a modal analysis concerning three different models (curved, straight and a combination of straight and curved beams) for a

vertically curved concrete flybridge. Based on the results obtained from the modal analysis, the combination of straight and curved beams at the cusp was suitable for VCCFBs because of their lower vehicle-induced vibrations, which were recorded at variable speeds. Talukdar and Roy (2019) studied the free in-plane vibration of a cracked curved beam with fixed ends based on Timoshenko beam theory. It was found that the natural frequency decreases with increasing crack depth. Also, the mode-shape results for the cracked beam showed a discontinuity at the crack location for displacements and rotations.

This work presents an extension of the method developed by El Kadiri et al. (2002) which has been carried out to study the geometrically non-linear response of thin straight structures with clamped or simply-supported ends. Indeed, this method has been used for the modal analysis of geometrically non-linear vibrations of various structures (El Hantati et al., 2022; El Khouddar et al., 2021; Outassafte et al., 2021). In this paper, the arch damage is modelled as a rotating elastic spring linking two adjacent arch sections. Also, this arch is assumed to be homogeneous, linearly elastic and the dimensions of its cross-section are considered small compared to the radius of curvature of the axis. The Euler-Bernoulli beam theory and the von-Kármán non-linear deformation assumptions are used to formulate a governing equation which predicts the free vibration. Hamilton's principle and an approximate method are used to solve the non-linear equation which governs different types of conditions. The present-method results are compared with those available in the literature. The good agreement noticed shows the efficiency and accuracy of this method. Several important aspects; namely, the effects of damage location, damage magnitude as well as the degree of damage, which affect the linear and non-linear vibration behavior, are investigated.

Mathematical Formulation

The Structural Model of a Damaged Arch

Considering a damaged circular arch as illustrated in Fig. 1, characterized by radius *R*, opening angle ϕ_0, location of a damage ϕ_D, Young's modulus E, cross-section A, moment of inertia *I* and distributed mass μ, the shear deformation and rotary inertia are neglected, because the arch is supposed to be thin. The section meaningful dimension is small compared with R and not shallow. Then, a standard assumption verified by numerical investigations is that the relevant behaviour of the arch is flexural.

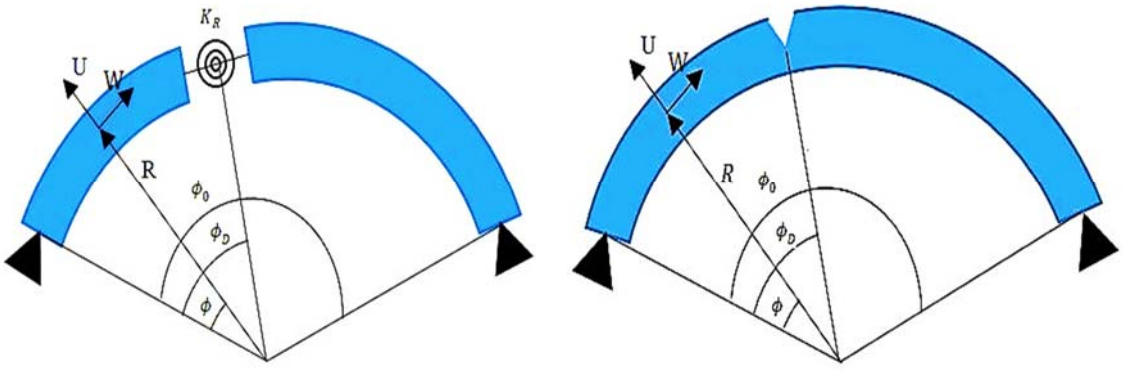

Figure (1): Modeling of a damaged circular arch simply supported with localized damage at $\phi = \phi_D$

The bending moment $M(\phi,t)$, the shear force $T(\phi,t)$ and the normal force $N(\phi,t)$ of the arch can be expressed as:

$$M(\phi,t) = \frac{-EI}{R^2}\left(\frac{\partial^3 w(\phi,t)}{\partial\phi^3} + \frac{\partial w(\phi,t)}{\partial\phi}\right) \quad (1)$$

$$T(\phi,t) = \frac{-1}{R^3}\frac{\partial}{\partial\phi}\left(EI(\phi)\frac{\partial^3 w(\phi,t)}{\partial\phi^3} + \frac{\partial w(\phi,t)}{\partial\phi}\right) \quad (2)$$

$$N(\phi,t)=\frac{-1}{R^3}\frac{\partial^2}{\partial\phi^2}\left[EI(\phi)\left(\frac{\partial^3 w(\phi,t)}{\partial\phi^3}+\frac{\partial w(\phi,t)}{\partial\phi}\right)\right]+\mu(\phi)R\frac{\partial^3 w(\phi,t)}{\partial\phi\partial t^2} \quad (3)$$

The simplified equation of motion is obtained after neglecting tangential and rotary inertia from Eqs. (1-3). The sixth-order differential equation of motion may be written as:

$$\frac{\partial^6 w(\phi,t)}{\partial\phi^6}+2\frac{\partial^4 w(\phi,t)}{\partial\phi^4}+\frac{\partial^2 w(\phi,t)}{\partial\phi^2}+\frac{\mu R^4}{EI}\frac{\partial^4 w(\phi,t)}{\partial\phi^2\partial t^2}=0 \quad (4)$$

Damage Modelization

The presence of damage in a structure may be due to a decrease in stiffness or a reduction in mass in an area either inside the structure, not visible except by non-destructive ultrasonic testing, or at the edge of the surface, which can be easily detected by using powder particles spread over the surface which will orientate differently from the damaged or discontinuous areas and will therefore be easily visualized, as well as by analyzing the values of vibration frequencies calculated by the analytical or numerical method.

In the model considered, the damaged zone has a cross-section of the same shape as the undamaged element, but with smaller dimensions.

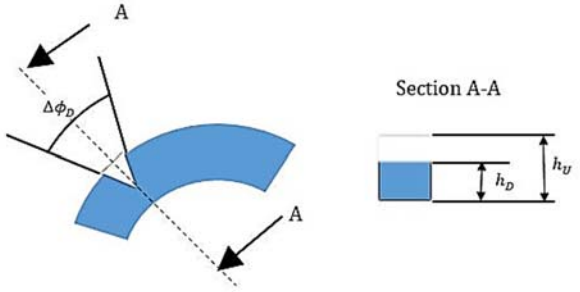

Figure (2): Damaged section of the arch

The stiffness at the damage is represented by an elastic rotational spring with stiffness K_R localized at angle ϕ_D. The value of K_R may be approximated supposing that the actual damage is distributed in a narrow zone of amplitude $\Delta\phi_D$ and that the average bending stiffness decrease in that zone is ΔEI. In analogy with the case of a rectilinear beam, it is possible to write that:

$$\gamma=\frac{(E_U I_U-E_D I_D)}{E_U I_U} \quad (5)$$

where $E_U I_U$ and $E_D I_D$ represent, respectively, the flexural stiffness of the undamaged and damaged cross-sections. The presence of a damage at the edge of the lateral surface can therefore be modelled by means of a rotating spring with the following stiffness (Cerri and Ruta, 2004):

$$K_R=\frac{(1-\gamma)}{\gamma}\frac{E_U I_U}{\Delta\phi_D} \quad (6)$$

Linear Vibration Formulation

Considering the arch in a harmonic motion, we put:

$$w(\phi,t)=W(\phi)\cos(\omega t) \quad (7)$$

If this form of solution is allowed:

$$W(\phi)=e^{\phi} \quad (8)$$

where $W(\phi)$ is the natural mode function of the spatial variable along the axis and ω is the natural circular frequency. Then, it is possible to arrive at this characteristic equation:

$$\Omega^6+2\Omega^4+(1-\lambda^2)\Omega^2=0 \quad (9)$$

where $\lambda_i^2=\mu^2R^4\omega_i^2/EI$ is the non-dimensional frequency. The radial displacement functions in the j^{th} span of the arch can be expressed as:

$$W(\phi)=\begin{cases}W_1(\phi)\longrightarrow]0,\phi_1[\\ \cdots\\ W_j(\phi)\longrightarrow]\phi_{j-1},\phi_j[\\ \cdots\\ W_{N+1}(\phi)\longrightarrow]\phi_N,1[\end{cases} \quad (10)$$

The general solution of the differential Eq. (9) in term of radial displacement in the j^{th} carck of the arch may be written as:

$$W_{ji}(\phi)=C_{1i}\sin\left(\alpha_i(\phi-\phi_{j-1})\right)+C_{2i}\cos\left(\alpha_i(\phi-\phi_{j-1})\right)+C_{3i}\sinh\left(\beta_i(\phi-\phi_{j-1})\right)+C_{4i}\cosh\left(\beta_i(\phi-\phi_{j-1})\right)+C_{5j}(\phi-\phi_{j-1})+C_{5j} \quad (11)$$

with

$$\alpha_i = \sqrt{\lambda_i - 1}\,, \quad \beta_i = \sqrt{\lambda_i - 1} \quad \text{and } \lambda_i \geq 1 \quad \text{pour } i = 1, \ldots, n \tag{12}$$

The boundary conditions are:

$$W_{1i}(\phi = 0) = W_{(N+1)i}(\phi = \phi_0) = 0 \tag{13}$$

$$\left.\frac{dW_i}{d\phi}\right|_{\phi=0} = \left.\frac{dW_{(N+1)i}}{d\phi}\right|_{\phi=\phi_0} = 0 \tag{14}$$

$$\left.\frac{d^3W_i}{d\phi^3}\right|_{\phi=0} = \left.\frac{d^3W_{(N+1)}}{d\phi^3}\right|_{\phi=\phi_0} = 0 \tag{15}$$

The compatibility conditions and continuity of each crack can be expressed as follows:

The continuity conditions at $\phi = \phi_j$:

$$W_{(j+1)i}(\phi = \phi_j) = W_{ji}(\phi = \phi_j) \tag{16}$$

Continuity of movement:

$$\left.\frac{dW_{(j+1)i}}{d\phi}\right|_{\phi=\phi_j} = \left.\frac{dW_{ji}}{d\phi}\right|_{\phi=\phi_j} \tag{17}$$

Continuity of rotation:

$$\left.\frac{d^3W_{(j+1)i}}{d\phi^3}\right|_{\phi=\phi_j} = \left.\frac{d^3W_{ji}}{d\phi^3}\right|_{\phi=\phi_j} \tag{18}$$

Continuity of bending moment:

$$\left.\left(\frac{d^2W_{(j+1)i}}{d\phi^2} + \frac{d^4W_{(j+1)i}}{d\phi^4}\right)\right|_{\phi=\phi_j} = \left.\left(\frac{d^2W_{ji}}{d\phi^2} + \frac{d^4W_{ji}}{d\phi^4}\right)\right|_{\phi=\phi_j} \tag{19}$$

Continuity of shear force:

$$\left.\frac{d^5W_{(j+1)i}}{d\phi^3}\right|_{\phi=\phi_j} = \left.\frac{d^5W_{ji}}{d\phi^3}\right|_{\phi=\phi_j} \tag{20}$$

The compatibility condition at $\phi = \phi_j$:

$$\left.\left(\frac{d^2W_{(j+1)i}}{d\phi^2} - \frac{d^4W_{(j+1)i}}{d\phi^4}\right)\right|_{\phi=\phi_j} = k_{ri}^* \left.\left(\frac{dW_{ji}}{d\phi} + \frac{d^3V_{ji}}{d\phi^3}\right)\right|_{\phi=\phi_j} \tag{21}$$

k_{ri}^* is the non-dimensional stiffness due to the damage related to the flexibility coefficient of the rotational spring by:

$$k_{ri}^* = \frac{K_{Ri}R^3}{EI} \tag{22}$$

Using the boundary conditions in Eqs. (13-15), the continuity condition at the crack and the compatibility due to rotational resort as written in Eqs. (16-21), the transfer matrix leads to a homogeneous system that has a non-triviality solution if the determinant is set equal to zero. The solution of the latest is determined iteratively by the Newton–Raphson algorithm. Then, the constants $C_{1j}, C_{2j}, C_{3j}, C_{4j} C_{5j}$ and C_{6j} are obtained by classical algebra.

Non-linear Vibration Formulation

The kinetic energy is denoted by *T*. The total strain energy of the system presented in Fig. 1 is denoted by V, written as a sum of the axial energy V_a, the strain energy due to bending V_b and the strain energy due to the damage V_D and can be expressed by:

$$T = \frac{R\mu}{2}\int_0^{\varphi_0}\left[\left(\frac{\partial w^{(1)}}{\partial t}\right)^2 + \left(\frac{\partial w}{\partial t}\right)^2\right]dt \tag{23}$$

$$V_a = \frac{EA}{8R^3}\int_0^{\varphi_0}\left(w + \frac{\partial^2 w}{\partial \phi^2}\right)^4 d\phi \tag{24}$$

$$V_b = \frac{EI}{2R^3}\int_0^{\varphi_0}\left(\frac{\partial w}{\partial \phi} + \frac{\partial^3 w}{\partial \phi^3}\right)^2 d\phi \tag{25}$$

$$V_D = \frac{(EI)^2}{2R^4K_R}\frac{\partial^2 w}{\partial \phi^2} + \left.\frac{\partial^4 w}{\partial \phi^4}\right|_{\phi=\phi_j} \tag{26}$$

with w_i being the tangential displacement of the arch and K_R the rigidity of the rotational spring. If the space and time functions are supposed to be separable and harmonic, motion is assumed. The tangential-displacement function is expanded in the form of finite basic spatial functions and can be written as:

$$w_i(\phi, t) = a_i W_i \sin(\omega t) \tag{27}$$

By replacing w_i in the energy expressions of T ,V_a, V_b and V_D, a new developed formulation can be written as:

$$T = \frac{1}{2} a_i a_j \omega^2 m_{ij} \cos^2(\omega t) \quad (28)$$

$$V_a = \frac{1}{2} a_i a_j a_k a_l \omega^2 b_{ijkl} \sin^4(\omega t) \quad (29)$$

$$V_b = \frac{1}{2} a_i a_j \, \omega^2 \mathrm{k}_{ij}^b \sin^2 \sin^2(\omega t) \quad (30)$$

$$V_D = \frac{1}{2} a_i a_j \mathrm{k}_{ij}^D \sin^2(\omega t) \quad (31)$$

The linear rigidities due to the bending strain and damage are denoted, respectively, by the parameters k_{ij}^b and k_{ij}^D. m_{ij} and b_{ijkl} represent, respectively, the mass tensor due to T and the quadratic non-linear rigidity tensor of the arch due to V_a. The k_{ij}^b, k_{ij}^D, m_{ij} and b_{ijkl} expressions are defined as:

$$m_{ij} = R\mu \int_0^{\phi_0} \left(\frac{\partial W_i}{\partial \phi} \frac{\partial W_j}{\partial \phi} + W_i W_j \right) d\phi \quad (32)$$

$$k_{ij}^b = \frac{EI}{R^3} \int_0^{\phi_0} \left(\frac{\partial W_i}{\partial \phi} + \frac{\partial^3 W_i}{\partial \phi^3} \right) \left(\frac{\partial W_j}{\partial \phi} + \frac{\partial^3 W_j}{\partial \phi^3} \right) d\phi \quad (33)$$

$$k_{ij}^D = \frac{(EI)^2}{R^4 K_R} \left(\frac{\partial^2 W_i}{\partial \phi^2} + \frac{\partial^4 W_i}{\partial \phi^4} \right)\Big|_{\phi=\phi_D} \left(\frac{\partial^2 W_j}{\partial \phi^2} + \frac{\partial^4 W_j}{\partial \phi^4} \right)\Big|_{\phi=\phi_D} \quad (34)$$

$$b_{ijkl} = \frac{EA}{R^3} \int_0^{\phi_0} \left(W_i + \frac{\partial^2 W_i}{\partial \phi^2} \right) \left(W_j + \frac{\partial^2 W_j}{\partial \phi^2} \right) \left(W_k + \frac{\partial^2 W_k}{\partial \phi^2} \right) \left(W_l + \frac{\partial^2 W_l}{\partial \phi^2} \right) d\phi \quad (35)$$

The coefficients a_i are unknowns as well as the frequency ω_i. The dynamic behavior of the conservative system may be obtained by applying Hamilton's principle as defined in Eq. (36):

$$\delta \int_0^{\frac{2\pi}{\omega}} (V_a + V_b + V_D - T) dt \quad (36)$$

The following non-linear algebraic equation can be obtained:

$$([K] - \omega^2 [M])\{A\} + \frac{3}{2}[B(A)]\{A\} = 0 \quad (37)$$

$\{A\}$ being the column vector of the basic function contribution coefficients. To simplify the analysis and the numerical treatment of the set of non-linear algebraic equations, a non-dimensional formulation has been considered by putting the spatial displacement function as:

$$W_i(\phi) = h W_i^*\left(\frac{\phi}{\phi_0}\right) = h W_i^*(\phi^*) \quad (38)$$

$$\frac{k_{ij}}{k_{ij}^*} = \frac{b_{ijkl}}{b_{ijkl}^*} = \frac{bh^2}{R^3} \quad (39)$$

$$\frac{m_{ij}}{m_{ij}^*} = bRh^2 \quad (40)$$

$$k_{ri} = \frac{K_R R^3}{EI} \quad (41)$$

where m_{ij}^*, k_{ij}^* and b_{ijkl}^* are the non-dimensional classical mass tensor, the linear rigidity tensor and the non-linear tensor, respectively, which are defined as:

$$m_{ij}^* = \int_0^1 \left(\frac{1}{\phi_0^2} \frac{\partial W_i^*}{\partial \phi^*} \frac{\partial W_j^*}{\partial \phi^*} + W_i^* W_j^* \right) \phi_0 d\phi \quad (42)$$

$$k_{ij}^* = \int_0^1 \left(\frac{1}{\phi_0} \frac{\partial W_i^*}{\partial \phi^*} + \frac{1}{{\phi_0}^3} \frac{\partial^3 W_i^*}{\partial \phi^{3*}} \right) \left(\frac{1}{\phi_0} \frac{\partial W_j^*}{\partial \phi^*} + \frac{1}{{\phi_0}^3} \frac{\partial^3 W_j^*}{\partial \phi^{3*}} \right) \phi_0 d\phi + \sum_{k=1}^{N} \left(\frac{1}{{\phi_0}^2} \frac{\partial^2 W_i^*}{\partial \phi^{*2}} + \frac{1}{{\phi_0}^4} \frac{\partial^4 W_i^*}{\partial \phi^{4*}} \right)\Big|_{\phi^*=\phi^*{}_k} \left(\frac{1}{{\phi_0}^2} \frac{\partial^2 W_j^*}{\partial \phi^{*2}} + \frac{1}{{\phi_0}^4} \frac{\partial^4 W_j^*}{\partial \phi^{4*}} \right)\Big|_{\phi^*=\phi^*{}_k} \quad (43)$$

$$b^*_{ijkl} = \alpha \int_0^1 \left(\frac{1}{\phi_0^2}\frac{\partial^2 W_i^*}{\partial \phi^{2*}} + W_i^*\right)\left(\frac{1}{\phi_0^2}\frac{\partial^2 W_j^*}{\partial \phi^{2*}} + W_j^*\right)\phi_0 d\phi^* \left(\frac{1}{\phi_0^2}\frac{\partial^2 W_k^*}{\partial \phi^{2*}} + W_k^*\right)\left(\frac{1}{\phi_0^2}\frac{\partial^2 W_l^*}{\partial \phi^{2*}} + W_i^*\right)\phi_0 d\phi^* \qquad (44)$$

For a uniform rectangular cross-section $\alpha = 3$, since in this case $({}^{h^2 S}/_{I} = 12)$. The functions W_i^* have been normalized in order to obtain that the mass matrix equals the identity matrix. The corresponding integrals defined in Eqs. (42-44) have been calculated using the Simpson's rule. By substituting the non-dimensional parameter in Eqs. (38-41) into Eq. (37), the dimensionless non-linear algebraic equation can be obtained and expressed as:

$$([K^*] - \omega^{*2}[M^*])\{A\} + \frac{3}{2}[B^*(\{A\})]\{A\} = 0 \qquad (45)$$

This equation appears as a generalization to the non-linear case of the classical linear free-response equation, very well known in linear modal analysis theory, where the term $\frac{3}{2}[B^*(\{A\})]\{A\}$ corresponding to the non-linear geometrical rigidity is added. ω^{*2} is the dimensionless non-linear frequency obtained by multiplying the left side of Equation (45) by $\{A\}^T$:

$$\omega^{*2} = \frac{\{A\}^T[K^*]\{A\} + k\{A\}^T[B^*(\{A\})]\{A\}}{\{A\}^T[M^*]\{A\}} \qquad (46)$$

with $k = {}^3/_2$.

The parameters m^*_{ij}. k^*_{ij} and b^*_{ijkl} have been numerically solved using Simpson's method in the range [0. 1] and the non-linear algebraic Eq. (45) has been solved using the second formulation.

Solution Methodology

To obtain non-linear beam mode shapes for higher amplitudes, the second formulation is an approximation which consists to separate the non-linear term of Eq. (45) into terms proportional to a_1^3 and terms proportional to $a_1^2\varepsilon_i$ and neglecting terms proportional to $a_1\varepsilon_i\varepsilon_j$ and terms proportional to $\varepsilon_i\varepsilon_j\varepsilon_k$. One can write:

$$a_i a_j a_k b^*_{ijkr} = a_1^3 b^*_{111r} + a_1^2 \varepsilon_i b^*_{11ir} \quad r = 1, \dots, n \qquad (47)$$

Using the tonsorial notation, one can put:

$$a_i k^*_{ir} + \frac{3}{2} a_i a_j a_k b^*_{ijkr} - a_i \omega^{*2} m^*_{ir} = 0 \quad r = 1, \dots, n \qquad (48)$$

After substituting and rearranging, Eq. (48) may be expressed in matrix form as:

$$([K^*_r]_R - \omega^2[M^*_r]_R)\{A_r\}_R + \frac{3}{2}[\alpha^*_r]_R\{A_r\}_R = \left\{-\frac{3}{2}a_r^3 b^*_{111r}\right\} \qquad (49)$$

in which $[K^*_r]_R = \left[k^*_{ij}\right]_R$ and $[M^*_r]_R = \left[m^*_{ij}\right]_R$ are reduced rigidity and mass matrices associated with the first non-linear mode obtained by varying i and j, $[\alpha^*_r]_R$ is a square matrix depending on a_1 whose general term α^*_{ij} is equal to $a_1^2 b^*_{11ir}$ and $a_1^3 b^*_{111r}$ is a column vector representing the right side of the non-linear system Eq. (49) in which the reduced unknown vector is $\{A_r\}_R = \{\varepsilon_2, \varepsilon_3, \dots, \varepsilon_r\}^T$. The modal contributions ε_i can be easily obtained by solving the non-linear system Eq. (49) of n equations and n unknowns. Higher non-linear mode shapes may be obtained in a similar manner, using an appropriate reduced matrix in each case. The non-linear frequency ω^{*2}_{nl} is given by:

$$\omega^{*2}_{nl} = \omega^{*2}_l + \frac{3}{2}\frac{b^*_{iiii}}{m^*_{ii}}a_i^2 \qquad \text{for} \qquad i = 1, \dots, n \qquad (50)$$

where ω^{*2}_l is the dimensionless linear natural frequency, which may be expressed as:

$$\omega^{*2}_l = \frac{k^*_{ii}}{m^*_{ii}} \qquad \text{for } i = 1, \dots, n \qquad (51)$$

The calculated contribution coefficients $\varepsilon_2, \dots, \varepsilon_n$ are included in Eq. (52) in order to calculate the normalized first non-linear mode $W^*_{nl1}(\phi^*, a_1)$. The normalized first non-linear deflection for a given value a_1 is then obtained as a series of basic functions involving the symmetrical terms $\varepsilon_3 W_3^*, \varepsilon_5 W_5^*, \dots, \varepsilon_9 W_9^*$ and is given by:

$$W^*_{nl1}(\phi^*, a_1) = a_1 W_1^* + \varepsilon_3 W_3^* + \varepsilon_5 W_5^* + \varepsilon_7 W_7^* + \varepsilon_9 W_9^* \qquad (52)$$

in which the predominant term proportional to the first linear mode shape $a_1 W_1^*$ and other terms proportional to higher modes $\varepsilon_3 W_3^*, \varepsilon_5 W_5^*, \dots, \varepsilon_9 W_9^*$ are the corrections due to non-linearity.

Numerical Results and Discussion for Linear Vibration

Comparative Studies and Validation of Results

To test the validity of results, relative variations of the first four frequencies *versus* the positions of damage have been calculated and compared with available data (Cerri and Ruta, 2004) which deals with the detection of localized damage in plane circular arches by frequency data. The geometrical and material properties considered are: the radius $R = 1000mm$, the opening angle $\phi_0 = {}^{2\pi}/_{3}$, the Young's modulus $E = 2 \times 10^5 N/mm^2$, the density $\rho = 7.87 \times 10^{-9} T/mm^3$ and having uniform rectangular cross-sections of base $b = 40mm$ and height $h = 20mm$. The damage was introduced by reducing the bending stiffness of three elements of the arch by $\Delta EI = 50\%$. This damage is localized, since the opening angle of the damaged zone is $\Delta\phi_D = {}^{\pi}/_{40}$.

Linear Vibration of Undamaged Circular Arch

A computer program has been written using MATLAB software to calculate the eigenvalues $\lambda_i = R^2\sqrt{{}^{\mu}/_{EI}}\,\omega_i$ $(i = 1,..,4)$ corresponding to thin undamaged circular arches $(k_r^* = \infty)$, hinged-hinged at both ends with the opening angle $\phi_0 = 20^o, 40^o, 80^o, 120^o, 160^o$ and 180^o. The results are presented in Table 1 and compared with those obtained by (De Rosa and Franciosi, 2000).

Table 1. The first four frequency parameters $\lambda_i = R^2\sqrt{{}^{\mu}/_{EI}}\,\omega_i$ $(i = 1,..,4)$, obtained for the undamaged simply supported circular arches

λ_i		$\phi_0 = 20^o$	$\phi_0 = 40^o$	$\phi_0 = 80^o$	$\phi_0 = 120^o$	$\phi_0 = 160^o$	$\phi_0 = 180^o$
λ_1	Present	323.0003	80.000	19.250	8.000	4.063	3.000
	(De Rosa and Franciosi, 2000)	323.0003	80.000	19.250	8.000	4.063	3.000
	DQM (De Rosa and Franciosi, 2000)	321.51482	78.55804	17.96407	6.92676	3.2179	2.26674
λ_2	Present	690.898	172.005	42.283	18.261	9.855	7.588
	(De Rosa and Franciosi, 2000)	690.898	172.005	42.283	18.261	9.855	7.588
	DQM (De Rosa and Franciosi, 2000)	690.04207	171.15800	41.46761	17.49631	9.1547	6.9233
λ_3	Present	1295.000	323.000	80.000	35.000	19.250	15.000
	(De Rosa and Franciosi, 2000)	1295.000	323.000	80.000	35.000	19.250	15.000
	DQM (De Rosa and Franciosi, 2000)	1293.51005	321.53908	78.64105	33.77403	18.16166	13.9777
λ_4	Present	1988.835	496.470	123.379	54.288	30.107	23.582
	(De Rosa and Franciosi, 2000)	1988.835	496.470	123.379	54.288	30.107	23.582
	DQM (De Rosa and Franciosi, 2000)	1987.97806	495.61730	122.54186	53.47580	29.32637	22.8196

Linear Vibration of Damaged Circular Arch

In order to validate the numerical results, a computer program has been written using MATLAB software to show how the parameters ${\phi_D}/{\phi_0}$ and k_r^* influence the natural frequencies of a damaged doubly hinged circular arch with an opening angle $\phi_0 = {}^{2\pi}/_{3}$. For each mode of this arch, the relative natural angular frequency variation is easily defined because of positions as ${\Delta\omega_i}/{\omega_i^U} = {(\omega_i^D - \omega_i^U)}/{\omega_i^U}) = 1 - {\lambda_i^D}/{\lambda_i^U}$; being calculated as a function of the damage parameters.

Fig. 3 shows the curves ${\Delta\omega_i}/{\omega_i^U}$ for the first four modes of vibration. As would be expected, the natural angular frequencies decrease with the degree of damage k_r^* and depend on the position of the localized damage along the axis of the arch. Furthermore, ${\Delta\omega_i}/{\omega_i^U}$

decreases with increasing k_r^*, attains a maximum when the damage is located at a peak value of the bending curvature while going to zero when the damage is located at a node of the bending curvature. Our comparison shows an excellent agreement with the results presented by Cerri and Ruta (2004) using the analytical approach.

The first four normalized transverse and longitudinal displacements of the hinged-hinged damaged circular arch are plotted in Fig. 4 and used below as basic functions in the non-linear analysis.

Fig. 5 shows the first four linear mode shapes of a simply supported damaged circular arch. As seen, the damaged zone is located at $\phi_D = {}^1/_3\,\phi_0$.

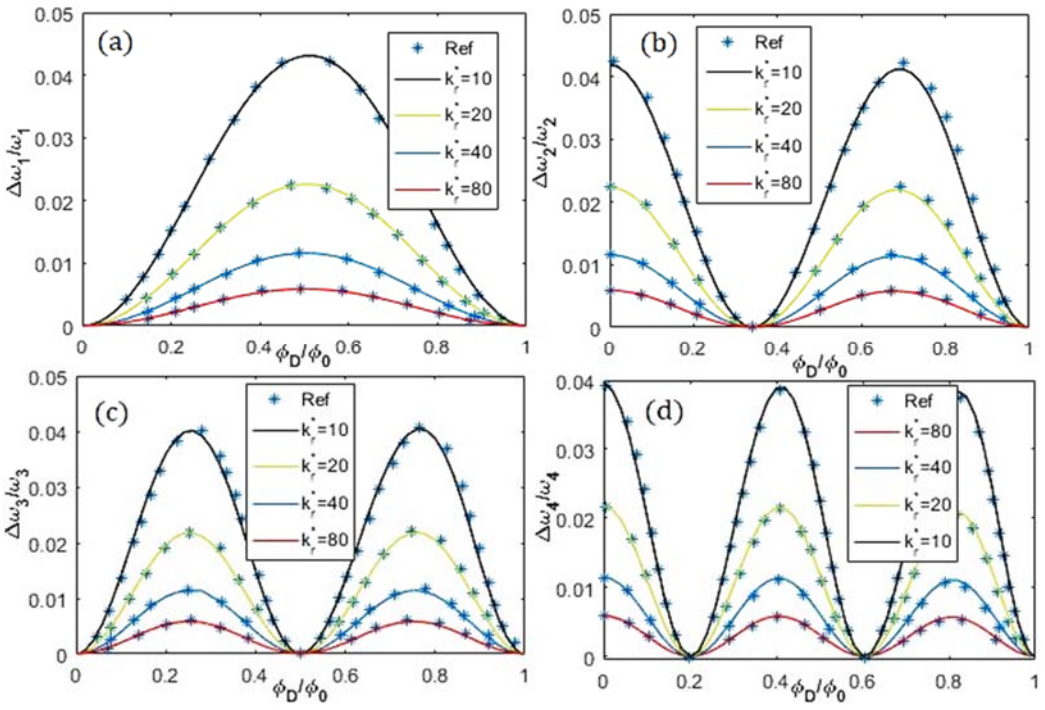

Figure (3): Variation of relative frequency ratios of the first four frequencies ${}^{\Delta\omega_i}/_{\omega_i^U}$ as a function of damage parameter k_r^* and ${}^{\phi_D}/_{\phi_0}$ with the results of Cerri and Ruta (2004). (a) first mode shape, (b) second mode shape, (c) third mode shape, (d) fourth mode shape

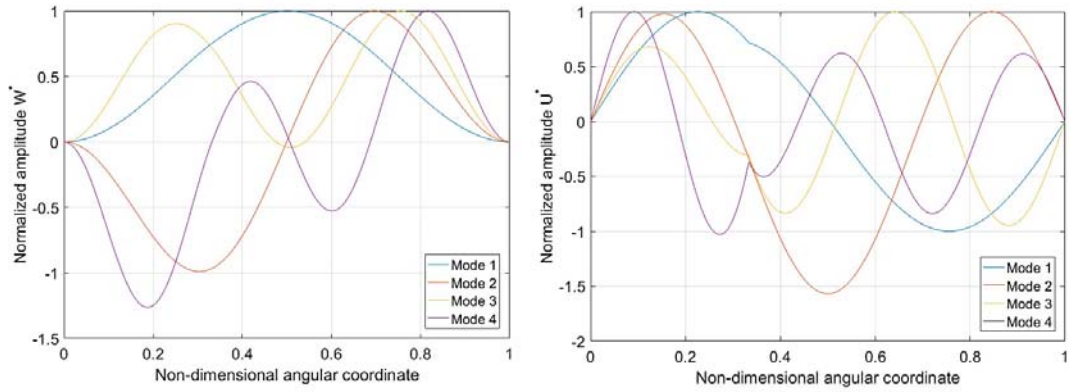

Figure (4): First four linear transverse and longitudinal displacements of a simply supported damaged circular arch

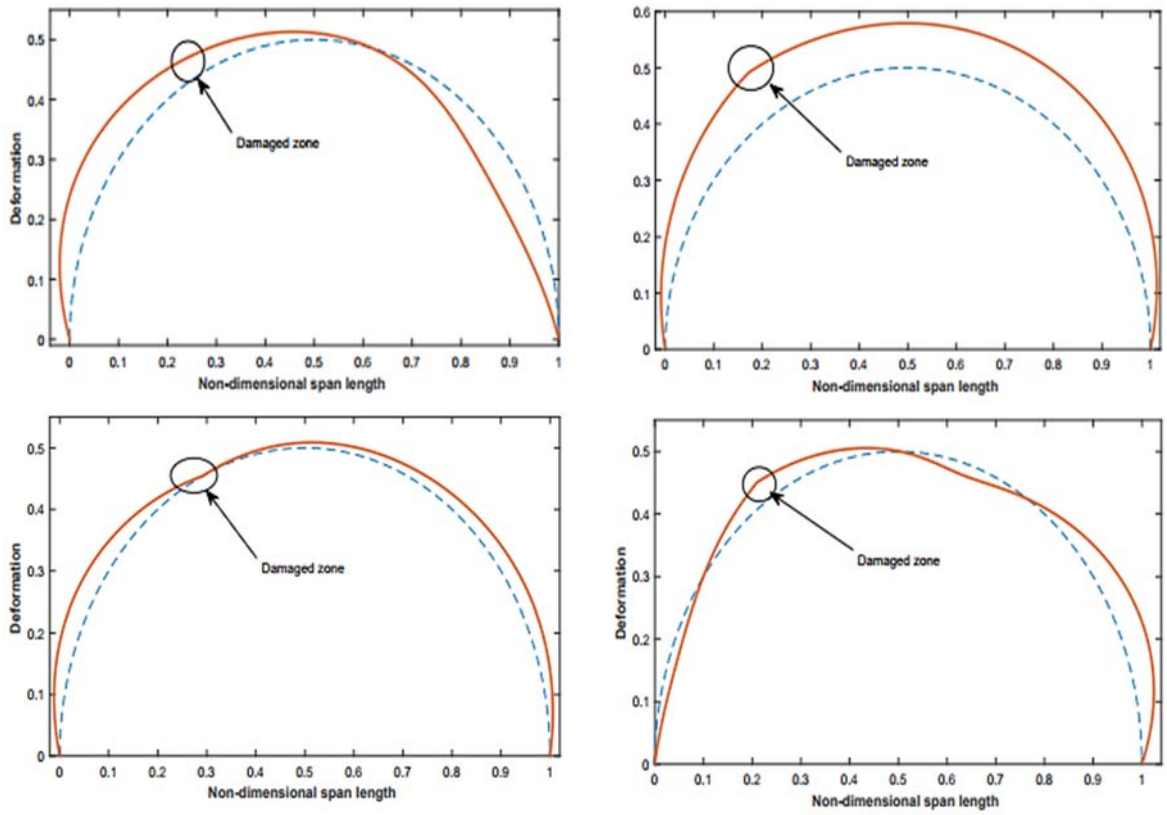

Figure (5): The first four mode shapes of a simply supported damaged circular arch

First natural frequency of the hinged-hinged arch with different numbers of damage is plotted in Fig 6 for various values of opening angle $\phi_0 = 80^o,\ 120^o,\ 160^o, 180^o$ and $k_r^* = 20$. We can observe that the increase in the number of cracks leads to an increase in the frequency.

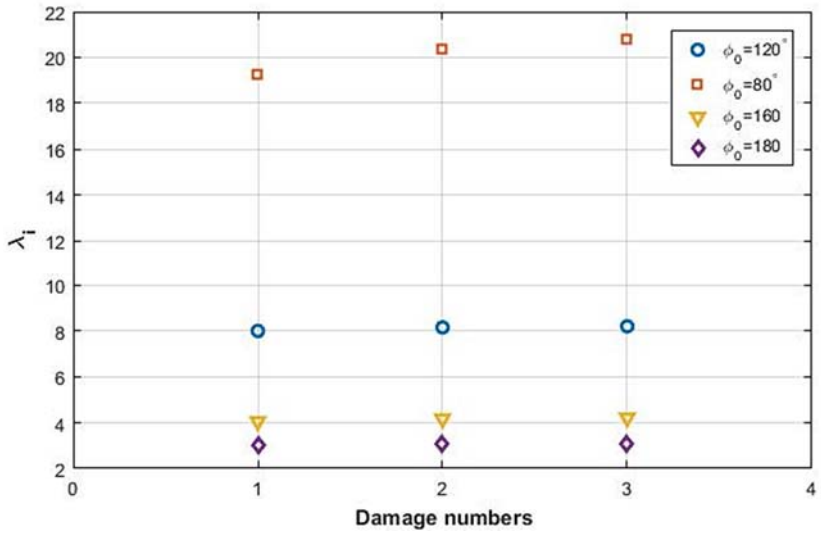

Figure (6): Variation of natural frequency with the number of damages

Numerical Results and Discussion for Non-linear Vibration of Damaged Circular Arch

The aim of this presented part is to show and analyze the effect of changing parameters, such as the damage location, the intensity and the number of the cracks, on the non-linear behavior of the simply supported damaged circular arch through the MATLAB program using the formulation obtained from Eq. (49). The basic contribution coefficients ε_i obtained by solving the non-linear algebraic system Eq. (49) are included into Eq. (52) to calculate the normalized first non-linear mode $W^*_{nl1}(\phi^*, a_1)$ of a hinged damaged circular arch. The maximum non-dimensional amplitude W^*_{max} represents the maximal value of the normalized first non-linear mode $W^*_{nl1}(\phi^*, a_1)$.

Effect of Opening Angle and Degree of Damage on Non-linear Vibration

Figures 7 (a-d) show the curves of the non-linear frequencies as a function of the maximum dimensionless vibration amplitude of the arch in the vicinity of the first mode. The effects of damage intensity on the non-linear dynamic behaviour of the arch for different values of the opening angle $\phi_0 = 80^o, 120^o, 160^o$ and 180^o are illustrated. The rotational spring that models the crack is placed at $\phi_D = {}^1\!/_3\,\phi_0$. It can be observed that the non-linear behaviour appears as a hardening type; the non-linear frequency increases as the vibration amplitude increases.

The numerical values of the linear and non-linear frequencies are summarized in Table 2 for the maximum non-dimensional amplitude $W^*_{max} = 1.5$. It can be seen from these results that increasing the stiffness of the rotational spring that models the damage leads to a decrease in the non-linear frequency of the arch. Therefore, we may say that the geometrical non-linearity of the arch is affected by the stiffness of the damage k^*_r.

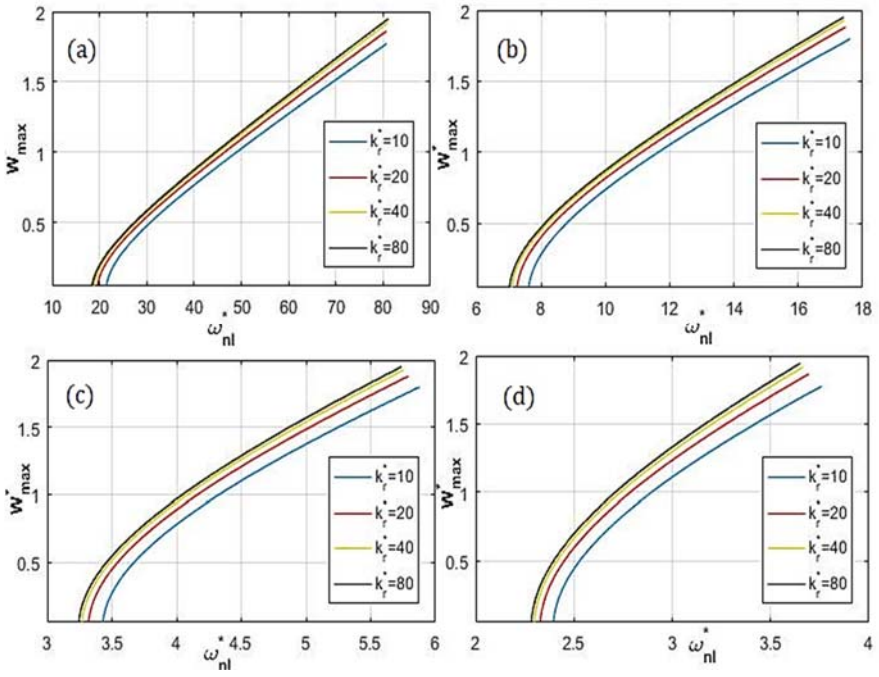

Figure (7): Non-linear frequency *versus* amplitude in the vicinity of the first mode shape for various values of the non-dimensional stiffness due to the damage k^*_r: (a) For an opening angle $\phi_0 = 80^o$, (b) For an opening angle $\phi_0 = 120^o$, (c) For an opening angle $\phi_0 = 160^o$ and (d) For an opening angle $\phi_0 = 180^o$

Table 2 shows that the dimensionless frequency decreases as the opening angle of the arch increases, but the rate of decrease is higher for small opening angles and very low for large opening angles. The decrease of the spring siftness increases by consequence of the hardening effect.

Table 2. Effect of rotational stiffness k_r^* and opening angle ϕ_0 on the linear and non-linear theory frequency of simply supported circular arch. Maximum non-dimensional amplitude W_{max}^*=1.5

$k_r^*=10$	$k_r^*=10$		$k_r^*=20$		$k_r^*=40$		$k_r^*=80$	
	ω_l^*	ω_{nl}^*	ω_l^*	ω_{nl}^*	ω_l^*	ω_{nl}^*	ω_l^*	ω_{nl}^*
$\phi_0=80^o$	21.38	69.45	19.48	66.21	18.72	64.05	18.42	63.38
Percentage of difference %	69.21		70.57		70.57		70.43	
$\phi_0=120^o$	7.62	15.22	7.26	14.61	7.10	14.27	7.016	14.10
Percentage of difference **%**	49.93		50.33		50.24		49.89	
$\phi_0=160^o$	3.43	5.24	3.31	5.03	3.26	4.92	3.24	4.87
Percentage of difference **%**	34.54		34.19		33,73		33.47	
$\phi_0=180^o$	2.38	3.43	2.32	3.27	2.29	3.20	2.28	3.16
Percentage of difference **%**	30.61		29.05		28,44		27.85	

Percentage of difference % = $\left|\frac{\omega_{nl}^*-\omega_l^*}{\omega_{nl}^*}\right| \times 100$.

Effects of the Number of Damages on Non-linear Vibration

As illustrated in Figure 8, three different cases of damaged circular arches with an opening angle ϕ_0=120º are investigated, after assigning the non-dimensional stiffness the following values k_r1^*=k_r1^*= k_r1^*=20. The three cases correspond to:

- Case 1: A circular arch with a single damage placed in the middle of the lateral surface.
- Case 2: A circular arch with two damages, each of which is distanced from the end of the arc by an angle of $\phi_0/_3$.
- Case 3: A circular arch with three damages, each of which is distant from the end of the arc by an angle of $\phi_0/_4$.

The effect of damage number on the non-linear behavior of a simply supported circular arch can be seen clearly in Fig. 9 giving the non-linear frequency dependence on the maximum dimensional vibration amplitude in the vicinity of the first non-linear mode shape for three considered cases as shown in Fig 8. It can be noticed that as the number of damages increases, the dimensionless non-linear frequencies increase. This effect is more pronounced with soft spring stiffness than with moderate and hard spring stiffnesses.

Table 4 presents the numerical values of the non-linear frequencies of a damaged circular arch with different values of the maximum dimensionless vibration amplitude and for the three cases considered, as shown in Figure 8. The results obtained show that the non-linear fundamental frequency is small for small amplitudes and becomes larger for moderate and higher amplitudes. This leads to the conclusion that the practical use of linear frequencies for small amplitudes can be of acceptable accuracy, given that it should limit the accuracy of the expected frequency estimate to a reasonable range.

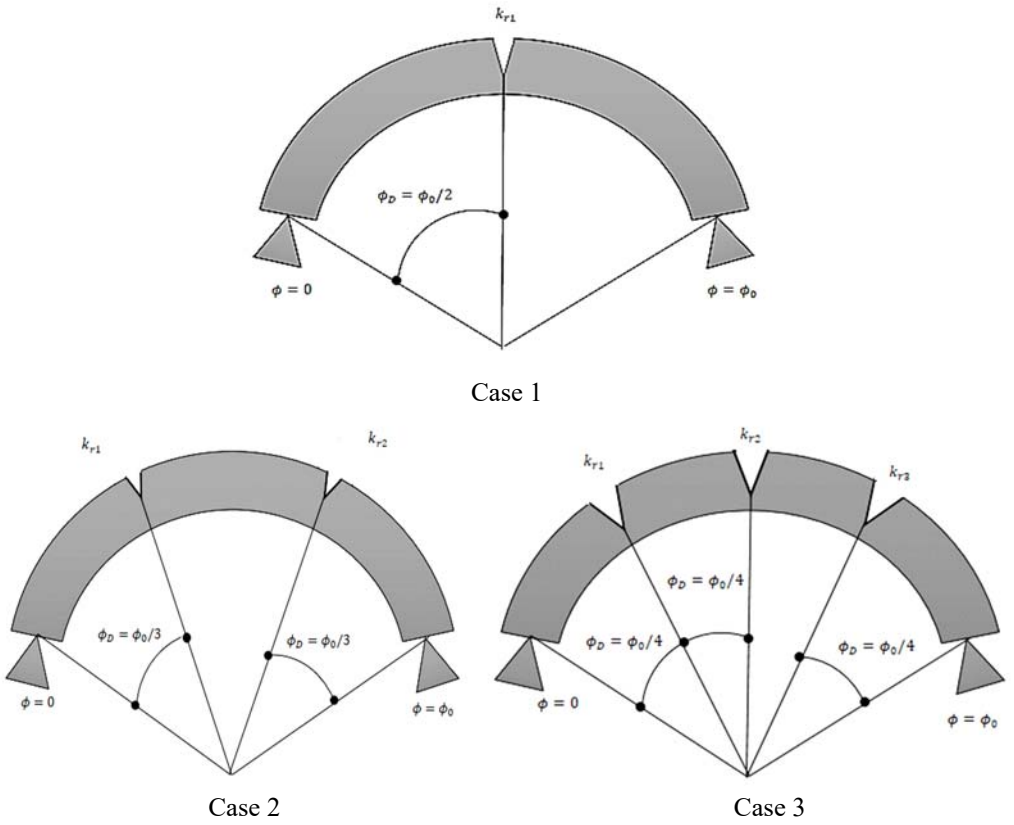

Figure (8): Configurations of a simply-supported circular arch: one damage (case 1), two damages (case 2) and three damages (case 3), where the opening angle $\phi_0 = 120^o$

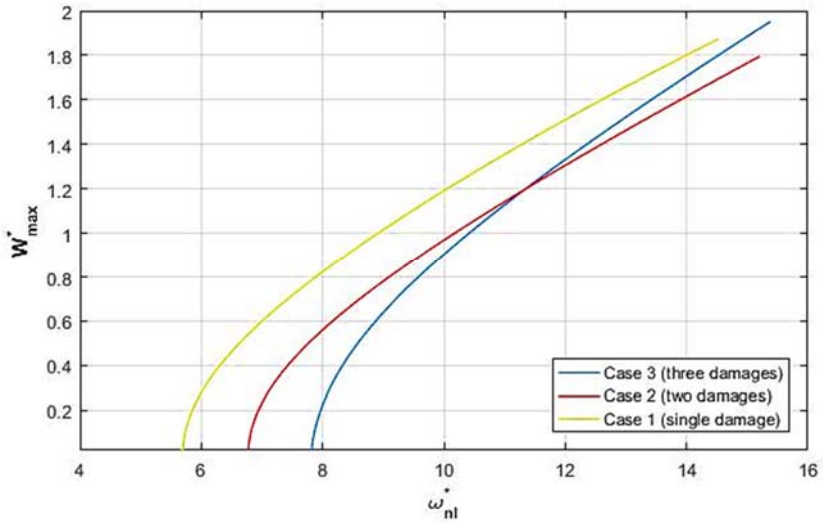

Figure (9): Non-linear frequency *versus* amplitude in the vicinity of the first mode shape for various numbers of rotational springs with ($\phi_0 = 120^o$ and $k^*_{r1} = k^*_{r1} = k^*_{r1} = 20^o$)

Table 3. Effect of damage numbers on the non-linear frequency ω_{nl}^* of hinged-hinged circular arch with various values of stiffness $k_r^* = k_{r1}^* = k_{r2}^* = k_{r3}^*$ for maximum non-dimensional amplitude W_{max}^*

W_{max}^*	Crack number	$k_r^* = 10$	$k_r^* = 20$	$k_r^* = 40$	$k_r^* = 80$
0.5	1	6.60	6.62	6.62	6.62
	2	8.48	7.78	7.57	7.46
	3	9.22	8.56	8.07	7.82
1	1	8.87	8.93	8.87	8.87
	2	11.10	10.15	10.09	9.86
	3	11.30	10.38	9.68	9.44
1.5	1	11.64	11.95	11.64	11.64
	2	14.55	12.90	13.21	12.97
	3	14.30	13.26	11.93	11.51

Effects of Damage Position on Non-linear Vibration

Figure 10 shows the effect of changing the position of the damage on the non-linear frequency-amplitude curves. It is remarkable that the non-linear frequency becomes higher when the damage is located in the centre of the arch. Therefore, we can say that the non-linear frequency of the arch is not only influenced by the number of damages, but also by other damage parameters, such as the damage position.

In other terms, we can deduce that the damage has more influence when it is located at the centre of the arch than when it is located at points considered as nodes.

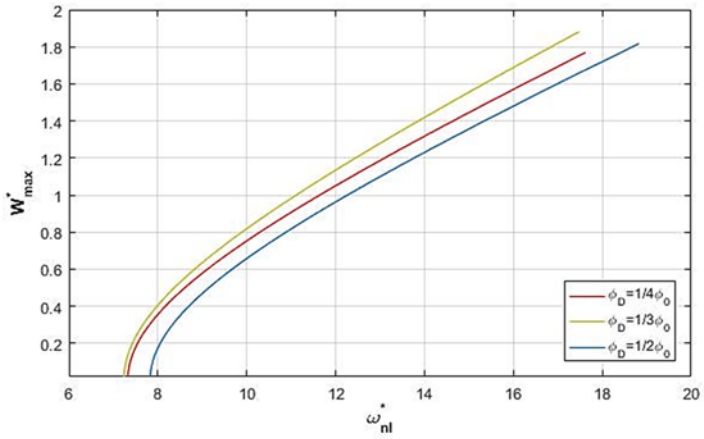

Figure (10): Non-linear frequency *versus* amplitude in the vicinity of the first mode shape, where the rotational spring is located at different positions $\phi_D = {}^1/_4\,\phi_0, {}^1/_3\,\phi_0, {}^1/_2\,\phi_0$ and ($\phi_0 = 120°$, $k_r^* = 20$)

Table 4. Effect of changing location of damage on the linear and non-linear theory frequency of hinged-hinged circular arch with a stiffness $k_r^* = 20$ and opening angle $\phi_0 = 120°$. Maximum non-dimensional amplitude $W_{max}^* = 1.5$

	$\phi_D = {}^1/_4\,\phi_0$	$\phi_D = {}^1/_3\,\phi_0$	$\phi_D = {}^1/_2\,\phi_0$
ω_l^*	7.32	7.23	7.82
ω_{nl}^*	15.45	14.61	16.2

Table 4 lists the numerical values of the linear and non-linear frequency of a simply supported circular arch with a damage located at different positions. These values are obtained by considering an opening angle of the arch of 120º and for a value of the dimensionless maximum vibration amplitude $W^*_{max} = 1.5$.

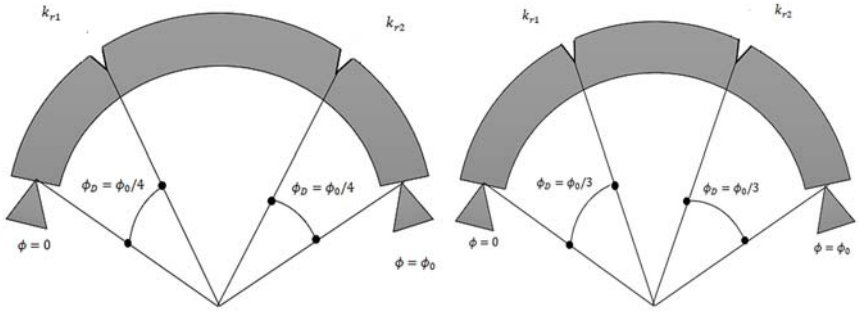

Case 4 Case 5

Figure (11): Configurations of a simply supported circular arch with two damages localized at different positions with ($\phi_0 = 120º$, $k^*_{r1} = k^*_{r2} = 20$)

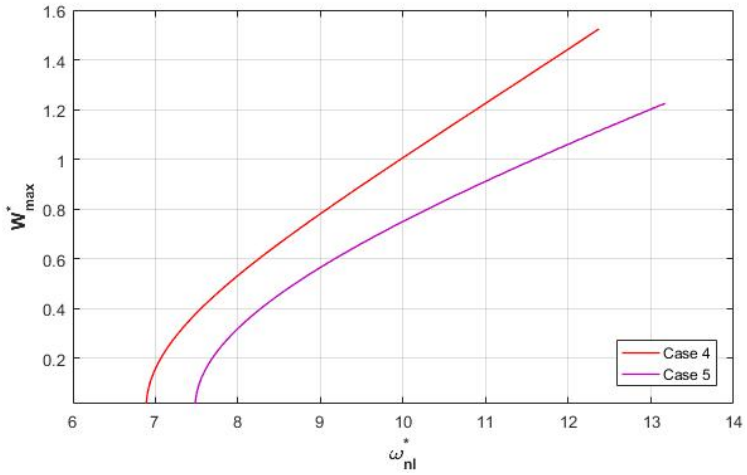

Figure (12): Non-linear frequency *versus* amplitude in the vicinity of the first mode shape for two damages located at different positions ($\phi_0 = 120º$, $k^*_{r1} = k^*_{r2} = 20$)

A comparison has been made in Figure 12 between two arcs containing two damages located at different places (as shown in Figure 11). In case 2, the damage is located closer to the ends of the arch, while in case 1, the damage is located further away from the ends of the arch. The results indicate that the damage further away from the arch ends has the least effect on non-linearity than the damage located near the arch ends.

CONCLUSIONS

Non-linear free vibration of a simply supported damaged circular arch has been studied and presented. The damage is modelled as an elastic rotational spring linking two adjacent sections. The generalized transcendent equation of frequency has been iteratively solved using the Newton-Raphson algorithm. The relative natural angular frequency variations have been calculated. The kinetic and total strain energies were discretized into a set of non-linear algebraic equations and derived using Hamilton's-principle energy and spectral analysis. The non-linear algebraic equation is obtained and numerically solved by an explicit method; the so-called second formulation. Based on multi-mode approach, the effects of the damage parameters, such as location, intensity of damage and number of damages, on the non-linear behavior of the arch were presented and discussed. Finally, the interesting results that can be

concluded from this work are listed as follows:

1. The presence of damages on an arch structure has a very significant effect on the behaviour of the spectral curves of the free dynamic response, where for different positions of the damages, different trends are observed.
2. The increase in the number of damages leads to an increase in the frequency of the structure. However, for an exiting frequency, the difference between the curves is insignificant for the high-amplitude region.
3. The effect of damage stiffness on the non-linear frequency is affected by the intensity of the stiffness and the number of damages. Indeed, the results show that increasing the stiffness and the number of damages leads to an increase in the frequency.

Funding

The authors received no financial support for conducting this research or for writing and/or publication of this article.

REFERENCES

Altunışık, A.C., Okur, F.Y., Karaca, S., and Kahya, V. (2019). "Vibration-based damage detection in beam structures with multiple cracks: Modal curvature *vs*. modal flexibility methods". Non-destructive Testing and Evaluation, 34, 33-53. https://doi.org/10.1080/10589759.2018.1518445.

Babahammou, A., and Benamar, R. (2020). "Semi-analytical solution of in-plane vibrations of circular arches carrying added point masses". Procedia-Manufacturing, 44, 465-472. https://doi.org/10.1016/j.promfg.2020.02.269.

Outassafte, O., Ahmed Adri, Yassine El Khouddar, Said Rifai, and Benamar, R. (2021). Geometrically non-linear free in-plane vibration of circular arch elastically restrained against rotation at the two ends". International Journal of Engineering Trends and Technology - IJETT.

Cerri, M.N., and Ruta, G.C. (2004). "Detection of localized damage in plane circular arches by frequency data". Journal of Sound and Vibration, 270, 39-59. https://doi.org/10.1016/S0022-460X(03)00482-6.

Cerri, M.N., Dilena, M., and Ruta, G.C. (2008). "Vibration and damage detection in undamaged and cracked circular arches: Experimental and analytical results". Journal of Sound and Vibration, 314, 83-94. https://doi.org/10.1016/j.jsv.2008.01.029.

Chondros, T.G., and Dimarogonas, A.D. (1980). "Identification of cracks in welded joints of complex structures". Journal of Sound and Vibration, 69, 531-538. https://doi.org/10.1016/0022-460X(80)90623-9.

Chondros, T.G., Dimarogonas, A.D., and Yao, J. (1998). "A continuous cracked beam vibration theory". Journal of Sound and Vibration, 215, 17-34. https://doi.org/10.1006/jsvi.1998.1640.

Christides, S., and Barr, A.D.S. (1984). "One-dimensional theory of cracked Bernoulli-Euler beams". International Journal of Mechanical Sciences, 26, 639-648. https://doi.org/10.1016/0020-7403(84)90017-1.

De Rosa, M.A., and Franciosi, C. (2000). "Exact and approximate dynamic analysis of circular arches using DQM". International Journal of Solids and Structures, 37, 1103-1117. https://doi.org/10.1016/S0020-7683(98)00275-3.

El Hantati, I., Adri, A., Fakhreddine, H., Rifai, S., and Benamar, R. (2022). "Multi-mode analysis of geometrically non-linear transverse free and forced vibrations of tapered beams". Shock and Vibration, 2022, e8464255. https://doi.org/10.1155/2022/ 8464255.

El Kadiri, M., Benamar, R., and White, R.G. (2002). "Improvement of the semi-analytical method for determining the geometrically non-linear response of thin straight structures- Part I: Application to clamped-clamped and simply supported-clamped beams". Journal of Sound and Vibration, 249, 263-305. https://doi.org/10.1006/jsvi.2001.3808.

El Khouddar, Y., Adri, A., Outassafte, O., Said, R., and Benamar, R. (2021). "An analytical approach to geometrically non-linear free and forced vibration of piezoelectric functional gradient beams resting on elastic foundations in thermal environments". Mechanics of Advanced Materials and Structures, 1-13. https://doi.org/10.1080/15376494.2021.2009601.

Irie, T., Yamada, G., and Tanaka, K. (1983). "Natural frequencies of in-plane vibration of arcs". Journal of Applied Mechanics, 50, 449-452. https://doi.org/10.1115/1.3167058.

Ja'E, I. (2018). "Vibration analysis of vertically curved concrete flyover bridges: Analytical model study". Jordan Journal of Civil Engineering, 12.

Khiem, N.T., and Lien, T.V. (2002). "The dynamic stiffness matrix method in forced vibration analysis of multiple-cracked beam". Journal of Sound and Vibration, 254, 541-555. https://doi.org/10.1006/jsvi.2001.4109.

Krawczuk, M., and Ostachowicz, W. (1997). "Natural vibrations of a clamped-clamped arch with an open transverse crack". Journal of Vibration and Acoustics, 119, 145-151. https://doi.org/10.1115/1.2889695.

Laura, P.A.A., and de Irassar, P.L.V. (1988). "A note on in-plane vibrations of arch-type structures of non-uniform cross-section: The case of linearly varying thickness". Journal of Sound and Vibration, 124, 1-12. https://doi.org/10.1016/S0022-460X(88)81402-0.

Liang, R.Y., Choy, F.K., and Hu, J. (1991). "Detection of cracks in beam structures using measurements of natural frequencies". Journal of the Franklin Institute, 328, 505-518. https://doi.org/10.1016/0016-0032(91)90023-V.

Outassafte, O., Adri, A., El Khouddar, Y., Rifai, S., and Benamar, R. (2021). "Geometrically non-linear free and forced vibration of a shallow arch". Journal of Vibroengineering, 23, 1508-1523. https://doi.org/10.21595/jve.2021.21857.

Papaeconomou, N., and Dimarogonas, A. (1989). "Vibration of cracked beams". Computational Mechanics, 88-94. https://doi.org/10.1007/BF01046 477.

Sinha, J.K., Friswell, M.I., and Edwards, S. (2002). "Simplified models for the location of cracks in beam structures using measured vibration data". Journal of Sound and Vibration 251, 13-38. https://doi.org/10.1006/jsvi.2001.3978.

Talukdar, S., and Roy, S.K. (2019). "Free in-plane vibration of a cracked curved beam with fixed ends". In: Advances in Engineering Design, A. Prasad, S.S. Gupta and R.K. Tyagi (eds.), Singapore: Springer Singapore, 363-376.

Tüfekçi, E. (2001). "Exact solution of free in-plane vibration of shallow circular arches". Int. J. Str. Stab. Dyn., 1, 409-428. https://doi.org/10.1142/S0219455401000226.

Yang, F., Sedaghati, R., and Esmailzadeh, E. (2018). "Free in-plane vibration of curved beam structures: A tutorial and the state-of-the-art". Journal of Vibration and Control, 24, 2400-2417. https://doi.org/10.1177/1077546317728148.

Zare, M. (2018). "On crack detection in curved beams using change of natural frequency". Journal of Vibroengineering, 20, 881-890. https://doi.org/10.21595/jve.2017.18774.

Zare, M. (2020). "Free out-of-plane vibration of cracked curved beams on elastic foundation by estimating the stress-intensity factor". Mechanics of Advanced Materials and Structures, 27, 1238-1245. https://doi.org/ 10.1080/15376494.2018.1506068.

Zhao, Y., and Kang, H. (2008). "In-plane free-vibration analysis of cable-arch structure". Journal of Sound and Vibration, 312, 363-379. https://doi.org/10.1016/j.jsv.2007.04.038.